

## Determination of the Strong Phase in $D^0 \rightarrow K^+ \pi^-$ Using Quantum-Correlated Measurements

J. L. Rosner,<sup>1</sup> J. P. Alexander,<sup>2</sup> D. G. Cassel,<sup>2</sup> J. E. Duboscq,<sup>2</sup> R. Ehrlich,<sup>2</sup> L. Fields,<sup>2</sup>  
 L. Gibbons,<sup>2</sup> R. Gray,<sup>2</sup> S. W. Gray,<sup>2</sup> D. L. Hartill,<sup>2</sup> B. K. Heltsley,<sup>2</sup> D. Hertz,<sup>2</sup>  
 C. D. Jones,<sup>2</sup> J. Kandaswamy,<sup>2</sup> D. L. Kreinick,<sup>2</sup> V. E. Kuznetsov,<sup>2</sup> H. Mahlke-Krüger,<sup>2</sup>  
 D. Mohapatra,<sup>2</sup> P. U. E. Onyisi,<sup>2</sup> J. R. Patterson,<sup>2</sup> D. Peterson,<sup>2</sup> D. Riley,<sup>2</sup> A. Ryd,<sup>2</sup>  
 A. J. Sadoff,<sup>2</sup> X. Shi,<sup>2</sup> S. Stroiney,<sup>2</sup> W. M. Sun,<sup>2</sup> T. Wilksen,<sup>2</sup> S. B. Athar,<sup>3</sup> R. Patel,<sup>3</sup>  
 J. Yelton,<sup>3</sup> P. Rubin,<sup>4</sup> B. I. Eisenstein,<sup>5</sup> I. Karliner,<sup>5</sup> S. Mehrabyan,<sup>5</sup> N. Lowrey,<sup>5</sup>  
 M. Selen,<sup>5</sup> E. J. White,<sup>5</sup> J. Wiss,<sup>5</sup> R. E. Mitchell,<sup>6</sup> M. R. Shepherd,<sup>6</sup> D. Besson,<sup>7</sup>  
 T. K. Pedlar,<sup>8</sup> D. Cronin-Hennessy,<sup>9</sup> K. Y. Gao,<sup>9</sup> J. Hietala,<sup>9</sup> Y. Kubota,<sup>9</sup> T. Klein,<sup>9</sup>  
 B. W. Lang,<sup>9</sup> R. Poling,<sup>9</sup> A. W. Scott,<sup>9</sup> P. Zweber,<sup>9</sup> S. Dobbs,<sup>10</sup> Z. Metreveli,<sup>10</sup>  
 K. K. Seth,<sup>10</sup> A. Tomaradze,<sup>10</sup> J. Libby,<sup>11</sup> A. Powell,<sup>11</sup> G. Wilkinson,<sup>11</sup> K. M. Ecklund,<sup>12</sup>  
 W. Love,<sup>13</sup> V. Savinov,<sup>13</sup> A. Lopez,<sup>14</sup> H. Mendez,<sup>14</sup> J. Ramirez,<sup>14</sup> J. Y. Ge,<sup>15</sup>  
 D. H. Miller,<sup>15</sup> B. Sanghi,<sup>15</sup> I. P. J. Shipsey,<sup>15</sup> B. Xin,<sup>15</sup> G. S. Adams,<sup>16</sup> M. Anderson,<sup>16</sup>  
 J. P. Cummings,<sup>16</sup> I. Danko,<sup>16</sup> D. Hu,<sup>16</sup> B. Moziak,<sup>16</sup> J. Napolitano,<sup>16</sup> Q. He,<sup>17</sup> J. Insler,<sup>17</sup>  
 H. Muramatsu,<sup>17</sup> C. S. Park,<sup>17</sup> E. H. Thorndike,<sup>17</sup> F. Yang,<sup>17</sup> M. Artuso,<sup>18</sup> S. Blusk,<sup>18</sup>  
 S. Khalil,<sup>18</sup> J. Li,<sup>18</sup> R. Mountain,<sup>18</sup> S. Nisar,<sup>18</sup> K. Randrianarivony,<sup>18</sup> N. Sultana,<sup>18</sup>  
 T. Skwarnicki,<sup>18</sup> S. Stone,<sup>18</sup> J. C. Wang,<sup>18</sup> L. M. Zhang,<sup>18</sup> G. Bonvicini,<sup>19</sup> D. Cinabro,<sup>19</sup>  
 M. Dubrovin,<sup>19</sup> A. Lincoln,<sup>19</sup> J. Rademacker,<sup>20</sup> D. M. Asner,<sup>21</sup> K. W. Edwards,<sup>21</sup>  
 P. Naik,<sup>21</sup> R. A. Briere,<sup>22</sup> T. Ferguson,<sup>22</sup> G. Tatishvili,<sup>22</sup> H. Vogel,<sup>22</sup> and M. E. Watkins<sup>22</sup>

(CLEO Collaboration)

<sup>1</sup>*Enrico Fermi Institute, University of Chicago, Chicago, Illinois 60637, USA*

<sup>2</sup>*Cornell University, Ithaca, New York 14853, USA*

<sup>3</sup>*University of Florida, Gainesville, Florida 32611, USA*

<sup>4</sup>*George Mason University, Fairfax, Virginia 22030, USA*

<sup>5</sup>*University of Illinois, Urbana-Champaign, Illinois 61801, USA*

<sup>6</sup>*Indiana University, Bloomington, Indiana 47405, USA*

<sup>7</sup>*University of Kansas, Lawrence, Kansas 66045, USA*

<sup>8</sup>*Luther College, Decorah, Iowa 52101, USA*

<sup>9</sup>*University of Minnesota, Minneapolis, Minnesota 55455, USA*

<sup>10</sup>*Northwestern University, Evanston, Illinois 60208, USA*

<sup>11</sup>*University of Oxford, Oxford OX1 3RH, UK*

<sup>12</sup>*State University of New York at Buffalo, Buffalo, New York 14260, U SA*

<sup>13</sup>*University of Pittsburgh, Pittsburgh, Pennsylvania 15260, USA*

<sup>14</sup>*University of Puerto Rico, Mayaguez, Puerto Rico 00681*

<sup>15</sup>*Purdue University, West Lafayette, Indiana 47907, USA*

<sup>16</sup>*Rensselaer Polytechnic Institute, Troy, New York 12180, USA*

<sup>17</sup>*University of Rochester, Rochester, New York 14627, USA*

<sup>18</sup>*Syracuse University, Syracuse, New York 13244, USA*

<sup>19</sup>*Wayne State University, Detroit, Michigan 48202, USA*

<sup>20</sup>*University of Bristol, Bristol BS8 1TL, UK*

<sup>21</sup>*Carleton University, Ottawa, Ontario, Canada K1S 5B6*

<sup>22</sup>*Carnegie Mellon University, Pittsburgh, Pennsylvania 15213, USA*

(Dated: February 14, 2008)

## Abstract

We exploit the quantum coherence between pair-produced  $D^0$  and  $\bar{D}^0$  in  $\psi(3770)$  decays to study charm mixing, which is characterized by the parameters  $x$  and  $y$ , and to make a first determination of the relative strong phase  $\delta$  between  $D^0 \rightarrow K^+\pi^-$  and  $\bar{D}^0 \rightarrow K^+\pi^-$ . Using 281 pb $^{-1}$  of  $e^+e^-$  collision data collected with the CLEO-c detector at  $E_{\text{cm}} = 3.77$  GeV, as well as branching fraction input from other experiments, we find  $\cos \delta = 1.03_{-0.17}^{+0.31} \pm 0.06$ , where the uncertainties are statistical and systematic, respectively. By further including other mixing parameter measurements, we obtain an alternate measurement of  $\cos \delta = 1.10 \pm 0.35 \pm 0.07$ , as well as  $x \sin \delta = (4.4_{-1.8}^{+2.7} \pm 2.9) \times 10^{-3}$  and  $\delta = (22_{-12}^{+11+9})^\circ$ .

The phenomenon of charm mixing is conventionally described by two small parameters,  $x \equiv (M_2 - M_1)/\Gamma$  and  $y \equiv (\Gamma_2 - \Gamma_1)/2\Gamma$ , where  $M_{1,2}$  and  $\Gamma_{1,2}$  are the masses and widths, respectively, of the  $CP$ -odd ( $D_1$ ) and  $CP$ -even ( $D_2$ ) neutral  $D$  meson mass eigenstates, and  $\Gamma \equiv (\Gamma_1 + \Gamma_2)/2$ . Many previous searches for charm mixing have used  $D^0$  decay times to attain first-order sensitivity to  $y$ . Lifetimes of  $D^0$  decays to  $CP$  eigenstates determine  $y$ , while doubly Cabibbo-suppressed (DCS) transitions probe  $R_M \equiv (x^2 + y^2)/2$  and a mode-dependent quantity,  $y'$ . For the most widely used DCS mode,  $D^0 \rightarrow K^+\pi^-$ ,  $y' \equiv y \cos \delta - x \sin \delta$ , where  $-\delta$  is the phase of  $\langle K^+\pi^-|D^0\rangle/\langle K^+\pi^-|\bar{D}^0\rangle \equiv r e^{-i\delta}$ . We adopt a convention in which  $\delta$  corresponds to a strong phase, which vanishes in the  $SU(3)$  limit [1]. To date,  $\delta$  has not been measured, so measurements of  $y$  and  $y'$  have not been directly comparable. The magnitude  $r$  of the amplitude ratio is approximately 0.06.

In this Letter, we implement the method described in Ref. [2] for measuring  $y$  and  $\cos \delta$  using quantum correlations at the  $\psi(3770)$  resonance [1, 3], where  $D^0\bar{D}^0$  pairs produced in  $e^+e^-$  collisions are in a  $C$ -odd eigenstate. We extract these parameters from decay rates to single tags (ST), which are individually reconstructed  $D^0$  or  $\bar{D}^0$  candidates, and double tags (DT), which are events where both  $D^0$  and  $\bar{D}^0$  are reconstructed.  $CP$  violation in  $D$  and  $K$  decays are negligible second order effects.

To first order in  $x$  and  $y$ , the rate  $\Gamma_{D^0\bar{D}^0}(i, j)$  for  $C$ -odd  $D^0\bar{D}^0$  decay to final state  $\{i, j\}$  follows from the anti-symmetric amplitude  $\mathcal{M}_{ij}$ :

$$\begin{aligned} \Gamma_{D^0\bar{D}^0}(i, j) &\propto \mathcal{M}_{ij}^2 = |A_i\bar{A}_j - \bar{A}_iA_j|^2 \\ &= |\langle i|D_2\rangle\langle j|D_1\rangle - \langle i|D_1\rangle\langle j|D_2\rangle|^2, \end{aligned} \quad (1)$$

where  $A_i \equiv \langle i|D^0\rangle$ ,  $\bar{A}_i \equiv \langle i|\bar{D}^0\rangle$ , and we have used  $|D_2\rangle = [|D^0\rangle \pm |\bar{D}^0\rangle]/\sqrt{2}$ . Using  $S_\pm$  and  $e^\pm$  to denote  $CP\pm$  eigenstates and semileptonic final states, respectively, these amplitudes are normalized such that  $\mathcal{B}_{K^-\pi^+} \approx A_{K^-\pi^+}^2(1 + ry \cos \delta + rx \sin \delta)$ ,  $\mathcal{B}_{S_\pm} \approx A_{S_\pm}^2(1 \mp y)$ , and  $\mathcal{B}_e \approx A_e^2$ . Quantum correlations affect neither the total  $D^0\bar{D}^0$  rate (and hence the number  $\mathcal{N}$  of  $D^0\bar{D}^0$  pairs produced) nor the ST rates. DT final states with pairs of  $CP$  eigenstates, however, are affected maximally; same- $CP$   $\{S_\pm, S_\pm\}$  states are forbidden, while opposite- $CP$   $\{S_+, S_-\}$  states are doubled in rate relative to uncorrelated decay. In general, the correlations introduce interference terms that can depend on  $y$  and  $\delta$ .

$D^0\bar{D}^0$  decay involving a final  $CP$  eigenstate naturally selects the  $D_1D_2$  basis. As a result, the branching fraction for an associated semileptonic decay probes  $y$ . While the semileptonic decay width itself does not depend on the  $CP$  eigenvalue, the total width of the parent  $D_1$  or  $D_2$  meson does:  $\Gamma_1 = \Gamma(1 \mp y)$ . Thus, the  $D_1$  semileptonic branching fraction is  $\mathcal{B}_e/(1 \mp y)$ , and the effective quantum-correlated  $D^0\bar{D}^0$  branching fraction ( $\mathcal{F}^{\text{cor}}$ ) for a  $\{S_\pm, e\}$  final state is  $\mathcal{F}_{S_\pm, e}^{\text{cor}} \approx 2\mathcal{B}_{S_\pm}\mathcal{B}_e(1 \pm y)$ , where the factor of 2 arises from the sum of  $e^+$  and  $e^-$  rates. When combined with estimates of  $\mathcal{B}_e$  and  $\mathcal{B}_{S_\pm}$  from ST yields, external sources, and flavor-tagged semileptonic yields, this equation allows  $y$  to be determined.

If an  $S_+$  and a  $K^-\pi^+$  decay occur in the same event, then the  $K^-\pi^+$  was produced by a  $D_1$ , and  $\mathcal{F}_{S_+, K\pi}^{\text{cor}}$  is

$$\begin{aligned} \mathcal{F}_{S_+, K\pi}^{\text{cor}} &= |\langle S_+|D_2\rangle\langle K^-\pi^+|D_1\rangle|^2 \\ &= A_{S_+}^2 |A_{K^-\pi^+} + \bar{A}_{K^-\pi^+}|^2 \\ &= A_{S_+}^2 A_{K^-\pi^+}^2 |1 + r e^{-i\delta}|^2 \\ &\approx \mathcal{B}_{S_+}\mathcal{B}_{K^-\pi^+}(1 + R_{\text{WS}} + 2r \cos \delta + y), \end{aligned} \quad (2)$$

where  $R_{\text{WS}}$  is the wrong-sign rate ratio, which depends on  $x$  and  $y$  because of the interference between DCS and mixing transitions:  $R_{\text{WS}} \equiv \Gamma(\bar{D}^0 \rightarrow K^- \pi^+)/\Gamma(D^0 \rightarrow K^- \pi^+) = r^2 + ry' + R_{\text{M}}$ . Similarly, the  $\{S_-, K\pi\}$  DT yield probes  $\mathcal{B}_{S_-} \mathcal{B}_{K^- \pi^+} (1 + R_{\text{WS}} - 2r \cos \delta - y)$ , and the asymmetry between these two DT yields gives  $\cos \delta$ , given knowledge of  $\mathcal{B}_{S_{\pm}}$ ,  $r$ , and  $y$ .

Table I shows  $\mathcal{F}^{\text{cor}}$  for all categories of final states considered in this analysis:  $K^{\mp} \pi^{\pm}$ ,  $S_{\pm}$ , and  $e^{\pm}$ . Comparison of  $\mathcal{F}^{\text{cor}}$  with the uncorrelated effective branching fractions,  $\mathcal{F}^{\text{unc}}$ , also given in Table I, provides  $r \cos \delta$ ,  $y$ ,  $r^2$ ,  $x^2$ , and  $rx \sin \delta$ . These five parameters are extracted by combining our ST and DT yields with external branching fraction measurements in a least-squares fit [4]. The external measurements, from incoherently produced  $D^0$  mesons, provide one measure of  $\mathcal{B}_i$ . The ST event yields provide a second measure; since each event has one  $D^0$  and one  $\bar{D}^0$ , inclusive rates correspond to uncorrelated branching fractions. The fit averages these estimates, and we extract updated  $\mathcal{B}_i$ . Finally, the DT/ST comparison provides  $\mathcal{N}$ , so the fit requires no knowledge of luminosity or  $D^0 \bar{D}^0$  production cross sections.

TABLE I: Correlated ( $C$ -odd) and uncorrelated effective  $D^0 \bar{D}^0$  branching fractions,  $\mathcal{F}^{\text{cor}}$  and  $\mathcal{F}^{\text{unc}}$ , to leading order in  $x$ ,  $y$ , and  $R_{\text{WS}}$ , divided by  $\mathcal{B}_i$  for ST modes  $i$  (first section) and  $\mathcal{B}_i \mathcal{B}_j$  for DT modes  $\{i, j\}$  (second section). Charge conjugate modes are implied.

| Mode                   | Correlated   | Uncorr.               |
|------------------------|--|-----------------------|
| $K^- \pi^+$            | $1 + R_{\text{WS}}$  | $1 + R_{\text{WS}}$   |
| $S_{\pm}$              | 2  | 2                     |
| $K^- \pi^+, K^- \pi^+$ | $R_{\text{M}}$   | $R_{\text{WS}}$       |
| $K^- \pi^+, K^+ \pi^-$ | $(1 + R_{\text{WS}})^2 - 4r \cos \delta (r \cos \delta + y)$ | $1 + R_{\text{WS}}^2$ |
| $K^- \pi^+, S_{\pm}$   | $1 + R_{\text{WS}} \pm 2r \cos \delta \pm y$                 | $1 + R_{\text{WS}}$   |
| $K^- \pi^+, e^-$       | $1 - ry \cos \delta - rx \sin \delta$                        | 1                     |
| $S_{\pm}, S_{\pm}$     | 0  | 1                     |
| $S_+, S_-$             | 4  | 2                     |
| $S_{\pm}, e^-$         | $1 \pm y$  | 1                     |

We analyze 281 pb $^{-1}$  of  $e^+e^-$  collision data produced by the Cornell Electron Storage Ring (CESR) at  $E_{\text{cm}} = 3.77$  GeV and collected with the CLEO-c detector, which is described in detail elsewhere [6]. We reconstruct the  $D^0$  and  $\bar{D}^0$  final states listed in Table II, with  $\pi^0/\eta \rightarrow \gamma\gamma$ ,  $\omega \rightarrow \pi^+\pi^-\pi^0$ , and  $K_S^0 \rightarrow \pi^+\pi^-$ . Signal and background efficiencies, as well as crossfeed probabilities among signal modes, are determined from simulated events that are processed in a fashion identical to data.

TABLE II:  $D$  final states reconstructed in this analysis.

| Type      | Final States   |
|-----------|--|
| Flavored  | $K^- \pi^+, K^+ \pi^-$                                 |
| $S_+$     | $K^+ K^-, \pi^+ \pi^-, K_S^0 \pi^0 \pi^0, K_L^0 \pi^0$ |
| $S_-$     | $K_S^0 \pi^0, K_S^0 \eta, K_S^0 \omega$                |
| $e^{\pm}$ | Inclusive $X e^+ \nu_e, X e^- \bar{\nu}_e$             |

The  $D$  candidate selection and yield determination procedures are described in a companion article [7] and are summarized below. Hadronic final states without  $K_L^0$  mesons are fully reconstructed via two kinematic variables: the beam-constrained candidate mass,

TABLE III: ST and DT yields, efficiencies, and their statistical uncertainties. For DT yields, we sum groups of modes and provide an average efficiency for each group; the number of modes in each group is given in parentheses. Modes with asterisks are not included in the standard and extended fits.

| Mode                             | Yield           | Efficiency (%)   |
|----------------------------------|-----------------|------------------|
| $K^-\pi^+$                       | $25374 \pm 168$ | $64.70 \pm 0.04$ |
| $K^+\pi^-$                       | $25842 \pm 169$ | $65.62 \pm 0.04$ |
| $K^+K^-$                         | $4740 \pm 71$   | $57.25 \pm 0.09$ |
| $\pi^+\pi^-$                     | $2098 \pm 60$   | $72.92 \pm 0.13$ |
| $K_S^0\pi^0\pi^0$                | $2435 \pm 74$   | $12.50 \pm 0.06$ |
| $K_S^0\pi^0$                     | $7523 \pm 93$   | $29.73 \pm 0.05$ |
| $K_S^0\eta$                      | $1051 \pm 43$   | $10.34 \pm 0.06$ |
| $K_S^0\omega$                    | $3239 \pm 63$   | $12.48 \pm 0.04$ |
| $K^\mp\pi^\pm, K^\mp\pi^\pm$ (2) | $4 \pm 2$       | $40.2 \pm 2.4$   |
| $K^-\pi^+, K^+\pi^-$ (1)         | $600 \pm 25$    | $41.1 \pm 0.2$   |
| $K^\mp\pi^\pm, S_+$ (8)          | $605 \pm 25$    | $26.1 \pm 0.1$   |
| $K^\mp\pi^\pm, S_-$ (6)          | $243 \pm 16$    | $12.3 \pm 0.1$   |
| $K^\mp\pi^\pm, e^\mp$ (2)        | $2346 \pm 65$   | $45.6 \pm 0.1$   |
| $S_+, S_+$ (9*)                  | $10 \pm 6$      | $12.5 \pm 0.6$   |
| $S_-, S_-$ (6*)                  | $2 \pm 2$       | $3.9 \pm 0.2$    |
| $S_+, S_-$ (12)                  | $242 \pm 16$    | $7.7 \pm 0.1$    |
| $S_+, e^\mp$ (6)                 | $406 \pm 44$    | $22.2 \pm 0.1$   |
| $S_-, e^\mp$ (6)                 | $538 \pm 40$    | $13.8 \pm 0.1$   |

$M \equiv \sqrt{E_0^2/c^4 - \mathbf{p}_D^2/c^2}$ , where  $\mathbf{p}_D$  is the  $D^0$  candidate momentum and  $E_0$  is the beam energy, and  $\Delta E \equiv E_D - E_0$ , where  $E_D$  is the sum of the  $D^0$  candidate daughter energies. We extract ST and DT yields from  $M$  distributions using unbinned maximum likelihood fits (ST) or by counting candidates in signal and sideband regions (DT).

Because most  $K_L^0$  mesons and neutrinos produced at CLEO-c are not detected, we only reconstruct modes with these particles in DTs, where the other  $D$  in the event is fully reconstructed. Ref. [8] describes the missing mass technique used to identify  $K_L^0\pi^0$  candidates. For semileptonic decays, we use inclusive, partial reconstruction to maximize efficiency, demanding only that the electron be identified. Electron identification utilizes a multivariate discriminant [9] that combines measurements from the tracking chambers, the electromagnetic calorimeter, and the ring imaging Čerenkov counter.

Table III gives yields and efficiencies for 8 ST modes and 58 DT modes, where the DT modes have been grouped into categories. Fifteen of the DT modes are forbidden by  $CP$  conservation and are not included in the nominal fits. In general, crossfeed among signal modes and backgrounds from other  $D$  decays are smaller than 1%. Modes with  $K_S^0\pi^0\pi^0$  have approximately 3% background, and yields for  $\{K^\mp\pi^\pm, K^\mp\pi^\pm\}$  and  $\{S_\pm, S_\pm\}$  are consistent with being entirely from background.

External inputs to the standard fit include measurements of  $R_M$ ,  $R_{WS}$ ,  $\mathcal{B}_{K^-\pi^+}$ , and  $\mathcal{B}_{S_\pm}$ , as well as an independent  $\mathcal{B}_{K_L^0\pi^0}$  from CLEO-c, as shown in Table IV.  $R_{WS}$  is required to constrain  $r^2$ , and thus, to convert  $r \cos \delta$  and  $rx \sin \delta$  to  $\cos \delta$  and  $x \sin \delta$ . We also perform an extended fit that uses the external mixing parameter measurements shown in Table V.

These fits incorporate the full covariance matrix for these inputs, accounting for statistical overlap with the yields in this analysis. Covariance matrices for the fits in Ref. [16] have been provided by the CLEO, Belle, and BABAR collaborations.

TABLE IV: Averages of external measurements used in the standard and extended fits. Charge-averaged  $D^0$  branching fractions are denoted by final state.

| Parameter                 | Average                    |
|---------------------------|----------------------------|
| $R_{\text{WS}}$           | $0.00409 \pm 0.00022$ [10] |
| $R_{\text{M}}$            | $0.00017 \pm 0.00039$ [11] |
| $K^- \pi^+$               | $0.0381 \pm 0.0009$ [12]   |
| $K^- K^+ / K^- \pi^+$     | $0.1010 \pm 0.0016$ [13]   |
| $\pi^- \pi^+ / K^- \pi^+$ | $0.0359 \pm 0.0005$ [13]   |
| $K_L^0 \pi^0$             | $0.0097 \pm 0.0003$ [8]    |
| $K_S^0 \pi^0$             | $0.0115 \pm 0.0012$ [12]   |
| $K_S^0 \eta$              | $0.00380 \pm 0.00060$ [12] |
| $K_S^0 \omega$            | $0.0130 \pm 0.0030$ [12]   |

TABLE V: Averages of external measurements used only in the extended fit.

| Parameter | Average                       |
|-----------|-------------------------------|
| $y$       | $0.00662 \pm 0.00211$ [13–15] |
| $x$       | $0.00811 \pm 0.00334$ [15]    |
| $r^2$     | $0.00339 \pm 0.00012$ [16]    |
| $y'$      | $0.0034 \pm 0.0030$ [16]      |
| $x'^2$    | $0.00006 \pm 0.00018$ [16]    |

Systematic uncertainties include those associated with efficiencies for reconstructing tracks,  $K_S^0$  decays,  $\pi^0$  decays, and for hadron identification (see Refs. [5, 7]). Other sources of efficiency uncertainty include:  $\Delta E$  requirements (0.5–5.5%),  $\eta$  reconstruction (4.0%), electron identification (1.0%), modeling of particle multiplicity and detector noise (0.1–1.3%), simulation of initial and final state radiation (0.5–1.2%), and modeling of resonant substructure in  $K_S^0 \pi^0 \pi^0$  (0.7%). We also include additive uncertainties of 0.0–0.9% to account for variations of yields with fit function.

These systematic uncertainties are included in the covariance matrix given to the fitter, which propagates them to the fit parameters. The other fit inputs determined in this analysis are ST and DT yields and efficiencies, crossfeed probabilities, background branching fractions and efficiencies, and statistical uncertainties on all of these measurements. Quantum correlations between signal and background modes are accounted for using assumed values of amplitude ratios and strong phases that are systematically varied and found to have negligible effect. We validated our analysis technique in a simulated  $C$ -odd  $D^0 \bar{D}^0$  sample 15 times the size of our data sample.

Table VI shows the results of the data fits, excluding the 15 same- $CP$  DT modes. Our standard fit includes the measurements in Table IV but not Table V. In this fit,  $x \sin \delta$  is

not determined reliably, so we fix it to zero, and the associated systematic uncertainty is  $\pm 0.03$  for  $\cos \delta$  and negligible for all other parameters. We obtain a first measurement of  $\cos \delta$ , consistent with being at the boundary of the physical region. Our branching fraction results do not supersede other CLEO-c measurements.

TABLE VI: Results from the standard fit (with Table IV inputs) and the extended fit (with Table IV/V inputs). Uncertainties are statistical and systematic, respectively. Charge-averaged  $D^0$  branching fractions are denoted by final state.

| Parameter                         | Standard Fit                | Extended Fit                |
|-----------------------------------|-----------------------------|-----------------------------|
| $\mathcal{N}$ ( $10^6$ )          | $1.042 \pm 0.021 \pm 0.010$ | $1.042 \pm 0.021 \pm 0.010$ |
| $y$ ( $10^{-3}$ )                 | $-45 \pm 59 \pm 15$         | $6.5 \pm 0.2 \pm 2.1$       |
| $r^2$ ( $10^{-3}$ )               | $8.0 \pm 6.8 \pm 1.9$       | $3.44 \pm 0.01 \pm 0.09$    |
| $\cos \delta$                     | $1.03 \pm 0.19 \pm 0.06$    | $1.10 \pm 0.35 \pm 0.07$    |
| $x^2$ ( $10^{-3}$ )               | $-1.5 \pm 3.6 \pm 4.2$      | $0.06 \pm 0.01 \pm 0.05$    |
| $x \sin \delta$ ( $10^{-3}$ )     | 0 (fixed)                   | $4.4 \pm 2.4 \pm 2.9$       |
| $K^- \pi^+$ (%)                   | $3.78 \pm 0.05 \pm 0.05$    | $3.78 \pm 0.05 \pm 0.05$    |
| $K^- K^+$ ( $10^{-3}$ )           | $3.87 \pm 0.06 \pm 0.06$    | $3.88 \pm 0.06 \pm 0.06$    |
| $\pi^- \pi^+$ ( $10^{-3}$ )       | $1.36 \pm 0.02 \pm 0.03$    | $1.36 \pm 0.02 \pm 0.03$    |
| $K_S^0 \pi^0 \pi^0$ ( $10^{-3}$ ) | $8.34 \pm 0.45 \pm 0.42$    | $8.35 \pm 0.44 \pm 0.42$    |
| $K_S^0 \pi^0$ (%)                 | $1.14 \pm 0.03 \pm 0.03$    | $1.14 \pm 0.03 \pm 0.03$    |
| $K_S^0 \eta$ ( $10^{-3}$ )        | $4.42 \pm 0.15 \pm 0.28$    | $4.42 \pm 0.15 \pm 0.28$    |
| $K_S^0 \omega$ (%)                | $1.12 \pm 0.04 \pm 0.05$    | $1.12 \pm 0.04 \pm 0.05$    |
| $X^- e^+ \nu_e$ (%)               | $6.54 \pm 0.17 \pm 0.17$    | $6.59 \pm 0.16 \pm 0.16$    |
| $K_L^0 \pi^0$ (%)                 | $1.01 \pm 0.03 \pm 0.02$    | $1.01 \pm 0.03 \pm 0.02$    |
| $\chi_{\text{fit}}^2/\text{ndof}$ | 30.1/46                     | 55.3/57                     |

The likelihood curve for  $\cos \delta$ , shown in Fig. 1a, is computed as  $\mathcal{L} = e^{-(\chi^2 - \chi_{\text{min}}^2)/2}$  at various fixed values of  $\cos \delta$ . It is highly non-Gaussian, so we assign asymmetric uncertainties (which still do not fully capture the non-linearity) by finding the values of  $\cos \delta$  where  $\Delta \chi^2 = 1$  to obtain  $\cos \delta = 1.03_{-0.17}^{+0.31} \pm 0.06$ . This non-linearity stems from the use of  $r \cos \delta$  to determine  $\cos \delta$ , which causes the uncertainty on  $\cos \delta$  to scale roughly like  $1/r$ . Because  $r^2$  is obtained from  $R_{\text{WS}}$ , an upward shift in  $y$  lowers the derived value of  $r^2$  (for positive  $r \cos \delta$ ), and the resultant uncertainty on  $\cos \delta$  increases, as illustrated by Fig. 1b. For values of  $|\cos \delta| < 1$ , we also compute  $\mathcal{L}$  as a function of  $|\delta|$ , and we integrate these curves within the physical region to obtain 95% confidence level (CL) limits of  $\cos \delta > 0.07$  and  $|\delta| < 75^\circ$ .

When combined with previous measurements of  $y$  and  $y'$ , our measurement of  $\cos \delta$  also gives  $x \sin \delta$ . Table VI shows the results of such an extended fit that includes external inputs from both Table IV and Table V. The resultant value of  $y$  includes the CLEO-c measurement from the standard fit, but the precision is dominated by the external  $y$  measurements. The overall uncertainty on  $\cos \delta$  increases to  $\pm 0.36$  because of the non-linearity discussed above. However, unlike the standard fit, the likelihood for  $\cos \delta$  is nearly Gaussian, as shown in Fig. 2a. The correlation coefficient between  $\cos \delta$  and  $x \sin \delta$  is 0.56, and we assign asymmetric uncertainties of  $x \sin \delta = (4.4_{-1.8}^{+2.7} \pm 2.9) \times 10^{-3}$ . By repeating the fit at various simultaneously fixed values of  $\cos \delta$  and  $\sin \delta$ , we also determine  $\delta = (22_{-12}^{+11+9})^\circ$ . The corresponding 95% CL intervals within the physical region are  $\cos \delta > 0.39$ ,  $x \sin \delta \in [0.002, 0.014]$ , and  $\delta \in [-7^\circ, +61^\circ]$ . Performing this extended fit with  $y$ ,  $x^2$ , and  $x \sin \delta$  fixed

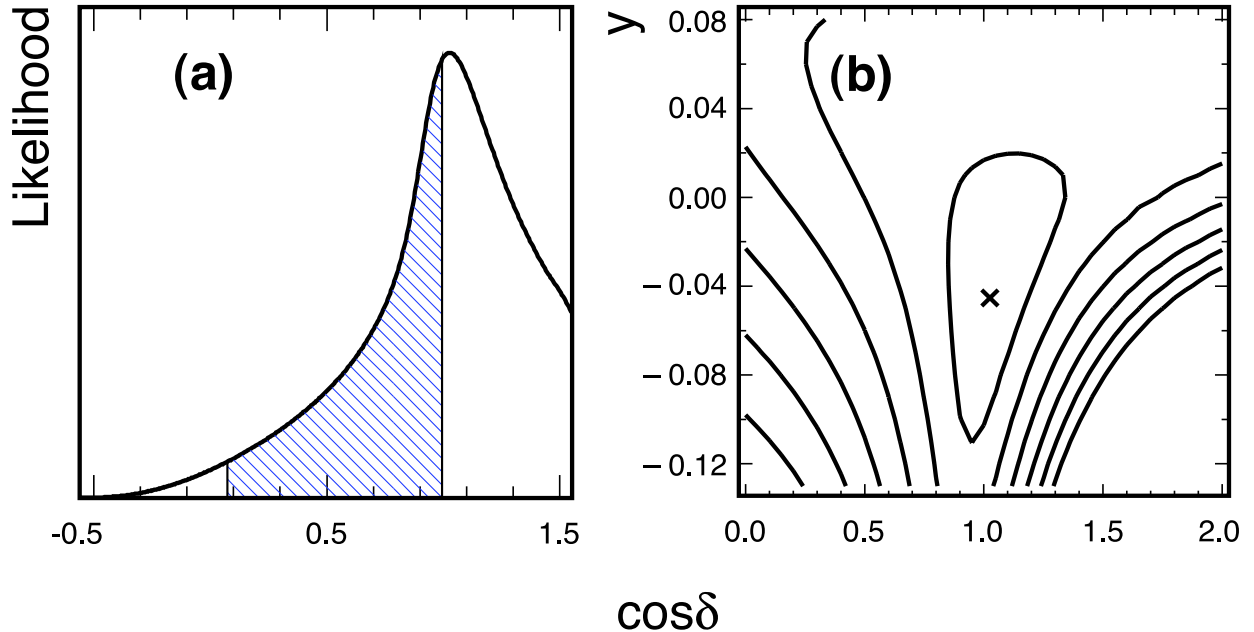


FIG. 1: Standard fit likelihood including both statistical and systematic uncertainties for  $\cos\delta$  (a), and simultaneous likelihood for  $\cos\delta$  and  $y$  (b) shown as contours in increments of  $1\sigma$ , where  $\sigma = \sqrt{\Delta\chi^2}$ . The hatched region contains 95% of the area in the physical region.

to zero results in a change in  $\chi^2$  of 25.1, or a significance of  $5.0\sigma$ .

By observing the change in  $1/\sigma_y^2$  as each fit input is removed, we identify the major contributors of information on  $y$  to be the  $\{S_\pm, e\}$  yields (90%) and  $\{K\pi, e\}$  yields (10%). For  $\cos\delta$ , the  $\{K\pi, S_\pm\}$  DT yields and the ST yields simultaneously account for 100%. We also find that no single input or group of inputs exerts a pull larger than  $3\sigma$  on  $\cos\delta$  or  $y$ . Moreover, removing all external inputs gives branching fractions consistent with those in Table IV. Finally, if we determine  $y$  only from  $K^+K^-$  and  $\pi^+\pi^-$  input, as in previous direct measurements, the result is consistent with the value in Table VI.

We also allow for a  $C$ -even  $D^0\bar{D}^0$  admixture in the initial state, which is expected to be  $\mathcal{O}(10^{-8})$  [18], by including the 15  $\{S_\pm, S_\pm\}$  DT yields in the fit. These modes limit the  $C$ -even component, which can modify the other yields as described in Ref. [2]. In both the standard and extended fits, we find a  $C$ -even fraction consistent with zero with an uncertainty of 2.4%, and neither the fitted parameters nor their uncertainties are shifted noticeably from the values in Table VI.

In summary, using  $281 \text{ pb}^{-1}$  of  $e^+e^-$  collisions produced at the  $\psi(3770)$ , we make a first determination of the strong phase  $\delta$ , with  $\cos\delta = 1.03_{-0.17}^{+0.31} \pm 0.06$ . By further including external mixing parameter measurements in our analysis, we obtain an alternate measurement of  $\cos\delta = 1.10 \pm 0.35 \pm 0.07$ , as well as  $x \sin\delta = (4.4_{-1.8}^{+2.7} \pm 2.9) \times 10^{-3}$  and  $\delta = (22_{-12}^{+11+9})^\circ$ .

We thank Alexey Petrov, William Lockman, Alan Schwartz, Bostjan Golob, and Brian Petersen for helpful discussions. We gratefully acknowledge the effort of the CESR staff in providing us with excellent luminosity and running conditions. This work was supported by the A.P. Sloan Foundation, the National Science Foundation, the U.S. Department of

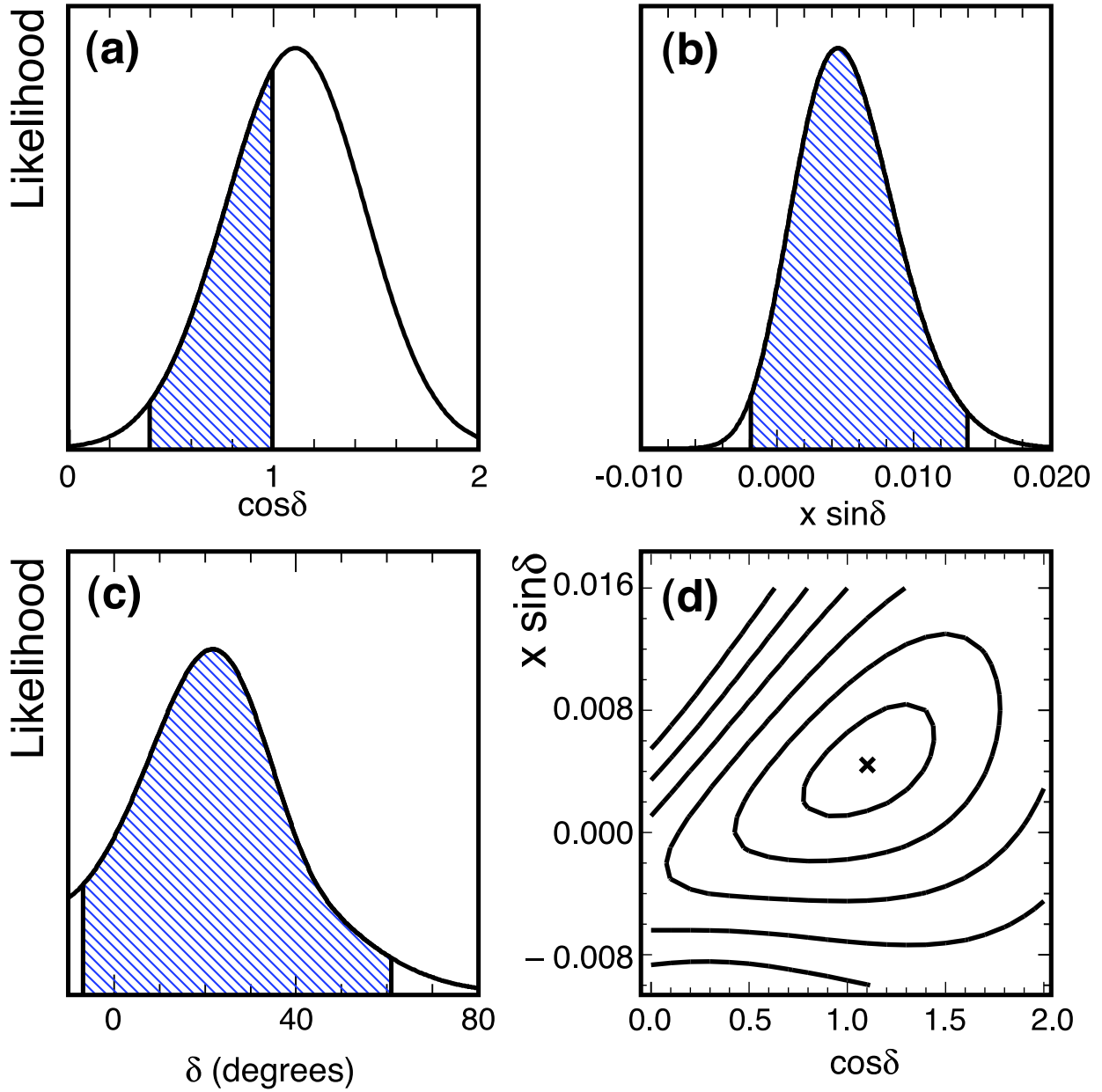


FIG. 2: Extended fit likelihood including both statistical and systematic uncertainties for  $\cos\delta$  (a),  $x \sin\delta$  (b),  $\delta$  (c), and simultaneous likelihood for  $\cos\delta$  and  $x \sin\delta$  (d) shown as contours in increments of  $1\sigma$ , where  $\sigma = \sqrt{\Delta\chi^2}$ . The hatched regions contain 95% of the area in the physical regions. For  $\delta$ , the fit fails to converge beyond the limits of the plot.

Energy, and the Natural Sciences and Engineering Research Council of Canada.

[1] M. Gronau, Y. Grossman and J. L. Rosner, Phys. Lett. B **508**, 37 (2001).

[2] D. M. Asner and W. M. Sun, Phys. Rev. D **73**, 034024 (2006) [Erratum-ibid. **77**, 019901(E)]

- (2008)].
- [3] R. L. Kingsley, S. B. Treiman, F. Wilczek and A. Zee, Phys. Rev. D **11**, 1919 (1975); L. B. Okun, B. M. Pontecorvo and V. I. Zakharov, Lett. Nuovo Cim. **13**, 218 (1975); R. L. Kingsley, Phys. Lett. B **63**, 329 (1976); M. Goldhaber and J. L. Rosner, Phys. Rev. D **15**, 1254 (1977); I. I. Bigi and A. I. Sanda, Phys. Lett. B **171**, 320 (1986); I. I. Bigi, SLAC-PUB-4000; I. I. Bigi, UND-HEP-89-BIG01, also SLAC-R-343, pp. 169–195; Z. Z. Xing, Phys. Rev. D **55**, 196 (1997); D. Atwood and A. A. Petrov, Phys. Rev. D **71**, 054032 (2005).
  - [4] W. M. Sun, Nucl. Instrum. Meth. A **556**, 325 (2006).
  - [5] S. Dobbs *et al.* [CLEO Collaboration], Phys. Rev. D **76**, 112001 (2007) [arXiv:0709.3783 [hep-ex]].
  - [6] Y. Kubota *et al.* [CLEO Collaboration], Nucl. Instrum. Methods Phys. Res., Sec. A **320**, 66 (1992); D. Peterson *et al.*, Nucl. Instrum. Methods Phys. Res., Sec. A **478**, 142 (2002); M. Artuso *et al.*, Nucl. Instrum. Methods Phys. Res., Sec. A **502**, 91 (2003); R.A. Briere *et al.* [CLEO-c/CESR-c Taskforces & CLEO-c Collaboration], Cornell LEPP preprint CLNS 01/1742 (2001).
  - [7] Companion paper, to be submitted to PRD.
  - [8] Q. He *et al.* [CLEO Collaboration], arXiv:0711.1463 [hep-ex].
  - [9] T. E. Coan *et al.* [CLEO Collaboration], Phys. Rev. Lett. **95**, 181802 (2005).
  - [10] E. M. Aitala *et al.* [E791 Collaboration], Phys. Rev. D **57**, 13 (1998); J. M. Link *et al.* [FOCUS Collaboration], Phys. Lett. B **618**, 23 (2005); A. Abulencia *et al.* [CDF Collaboration], Phys. Rev. D **74**, 031109 (2006).
  - [11] E. M. Aitala *et al.* [E791 Collaboration], Phys. Rev. Lett. **77**, 2384 (1996); C. Cawlfeld *et al.* [CLEO Collaboration], Phys. Rev. D **71**, 077101 (2005); K. Abe *et al.* [Belle Collaboration], Phys. Rev. D **72**, 071101 (2005); B. Aubert *et al.* [BABAR Collaboration], Phys. Rev. D **76**, 014018 (2007).
  - [12] S. Eidelman *et al.*, Phys. Lett. B **592**, 1 (2004).
  - [13] W.-M. Yao *et al.*, Journal of Physics G **33**, 1 (2006).
  - [14] M. Staric *et al.* [Belle Collaboration], Phys. Rev. Lett. **98**, 211803 (2007).
  - [15] D. M. Asner *et al.* [CLEO Collaboration], Phys. Rev. D **72**, 012001 (2005); L. M. Zhang *et al.* [BELLE Collaboration], Phys. Rev. Lett. **99**, 131803 (2007).
  - [16] R. Godang *et al.* [CLEO Collaboration], Phys. Rev. Lett. **84**, 5038 (2000); L. M. Zhang *et al.* [BELLE Collaboration], Phys. Rev. Lett. **96**, 151801 (2006); B. Aubert *et al.* [BABAR Collaboration], Phys. Rev. Lett. **98**, 211802 (2007).
  - [17] A. Abulencia *et al.* [CDF Collaboration], Phys. Rev. D **74**, 031109 (2006).
  - [18] A. Petrov, private communication.